

(Octaethylazaporphyrinato)iron(III) Chloride: Its Structure in the Solid State and in Solution[†]

Alan L. Balch,* Marilyn M. Olmstead, and Nasser Safari

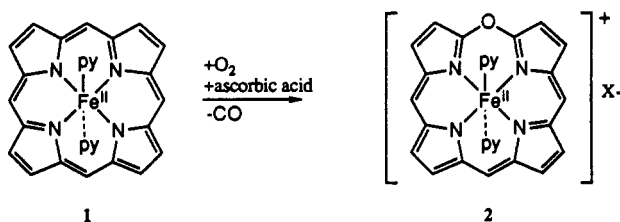
Department of Chemistry, University of California, Davis, California 95616

Received July 14, 1992

The structure of (OEAP)Fe^{III}Cl (where OEAP is the dianion of octaethylazaporphyrin), which was obtained from verdohemochrome by treatment with ammonia, was determined by X-ray crystallography. Red blocks of C₃₅H₄₃N₅-FeCl·CH₂Cl₂·N₂ form in the triclinic space group $P\bar{1}$ with $a = 10.051(2) \text{ \AA}$, $b = 13.746(3) \text{ \AA}$, $c = 14.712(3) \text{ \AA}$, $\alpha = 66.50(3)^\circ$, $\beta = 80.72(3)^\circ$, and $\gamma = 75.93(3)^\circ$ at 130 K with $Z = 2$. Refinement of 424 parameters with 3056 reflections gave $R = 0.071$, $R_w = 0.089$. The structure shows a typical high-spin five-coordinate iron with Fe-N(av) = 2.044 Å and the iron 0.49 Å out of the N₄ plane. A dichloromethane molecule is hydrogen bonded to the meso nitrogen in the solid. This interaction plays a role in ordering the structure of this symmetrically substituted, core-modified porphyrin. (OEAP)Fe^{III}Cl reacts with hydrogen chloride in dichloromethane to form high-spin, six-coordinate (HOEAP)Fe^{III}Cl₂. In this transformation, the ability of the meso nitrogen to accept a proton triggers a significant change in the coordination geometry of the iron. In dimethyl sulfoxide, (OEAP)Fe^{III}Cl reacts with silver nitrate to form high-spin [(OEAP)Fe^{III}(DMSO)₂](NO₃). These reactions have been monitored by UV/vis absorption and ¹H NMR spectroscopy.

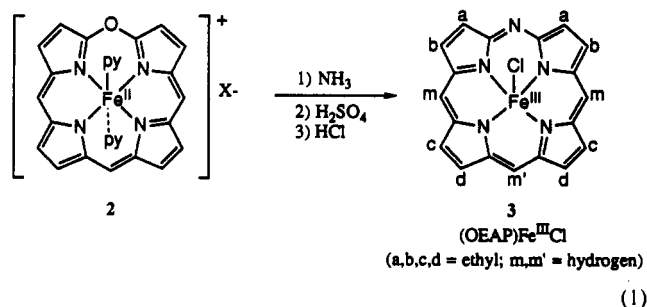
Introduction

Oxidation of iron(II) porphyrin **1** by dioxygen in pyridine in the presence of a reducing agent (ascorbic acid or hydrazine) produces a green compound **2** (verdohemochrome) that contains



the oxoporphyrin structure.¹⁻⁵ This process, which is called coupled oxidation, has been used as a model for biological heme degradation. Heme catabolism is a two-step process that is catalyzed by the enzymes heme oxygenase and biliverdin reductase. They convert heme to bilirubin and the bile pigments.⁶⁻⁸

Treatment of verdohemochrome in pyridine with ammonia in the presence of air followed by treatment with sulfuric acid and hydrogen chloride in methanol results in the formation of the azaporphyrin complex **3** (reaction 1).⁹⁻¹¹ This type of reaction, which converts the oxoporphyrin macrocycle into the azaporphyrin was historically significant because it was one of the early indications that verdohemochrome contained one less carbon atom than heme.^{1,9}



This article is concerned with structural characterization of **3** (with a, b, c, d = ethyl and m and m' = H) in the solid state and in solution. Metal complexes of azaporphyrin macrocycles have received very limited attention.¹⁰⁻¹² In order to fully characterize verdohemochrome and understand its chemical behavior, it was necessary to explore the nature of the azaporphyrin that was obtained from **3**.

Results

The red-brown, air-stable complex **3** was prepared from octaethylverdohemochrome (**2**) by a minor modification of the previously described route.¹¹ The electronic absorption spectrum obtained from a dichloromethane solution of the complex is shown in trace A of Figure 1. Spectral changes are seen when hydrogen chloride is added to this solution, as shown in trace B of Figure 1. Dissolution of the complex in dimethyl sulfoxide and treatment of that solution with silver nitrate (which produces a precipitate of silver chloride) give a solution whose absorption spectrum is shown in trace C of Figure 1. The procedure is well-known to form high-spin, six-coordinate porphyrin complexes in which the iron(III) is coordinated by two axial dimethyl sulfoxide ligands.¹³ Hence, the solution giving the spectrum shown in trace C contains [(OEAP)Fe^{III}(DMSO)₂](NO₃).

The magnetic properties of **3** indicate that it is a high-spin complex. The magnetic moment in dichloromethane solution is 5.7 (2) μ_B at 23 °C. The electron spin resonance spectrum in

[†] Abbreviations: OEP, dianion of octaethylporphyrin; OEAP, dianion of octaethylazaporphyrin; DMSO, dimethyl sulfoxide; py, pyridine.

- (1) Lemberg, R. *Rev. Pure Appl. Chem.* **1956**, *6*, 1.
- (2) Levin, E. Y. *Biochemistry* **1966**, *5*, 2845.
- (3) Saito, S.; Itano, H. A. *Proc. Natl. Acad. Sci. U.S.A.* **1982**, *79*, 1393.
- (4) Lagarias, J. C. *Biochem. Biophys. Acta* **1982**, *717*, 12.
- (5) Balch, A. L.; Latos-Grazyński, L.; Noll, B. C.; Olmstead, M. M.; Safari, N. *J. Am. Chem. Soc.*, in press.
- (6) Bissell, D. M. In *Bile Pigments and Jaundice*; Ostrow, J. D. Ed.; Liver: Normal Function and Disease, Vol. 4; Marcel Dekker, Inc.: New York, 1986; p 133.
- (7) Schmid, R.; McDonagh, A. F. In *The Porphyrins*; Dolphin, D., Ed.; Academic Press: New York, 1979; Vol. 6, p 258.
- (8) O'Carra, P. In *Porphyrins and Metalloporphyrins*; Smith, K. M., Ed.; Elsevier: New York, 1975; p 122.
- (9) Lemberg, R. *Aust. J. Exp. Biol. Med. Sci.* **1943**, *21*, 239.
- (10) Saito, S.; Tamura, N. *Bull. Chem. Soc. Jpn.* **1987**, *160*, 4037.
- (11) Saito, S.; Sumita, S.; Iwai, K.; Sano, H. *Bull. Chem. Soc. Jpn.* **1988**, *61*, 3539.

- (12) Abeyskera, A. M.; Grigg, R.; Malone, J. F.; King, T. J.; Morely, J. O. *J. Chem. Soc., Perkin Trans. 2* **1985**, 395.
- (13) Budd, D. L.; La Mar, G. N.; Langry, K. C.; Smith, K. M.; Mayyir-Mazhir, R. *J. Am. Chem. Soc.* **1979**, *101*, 6091.

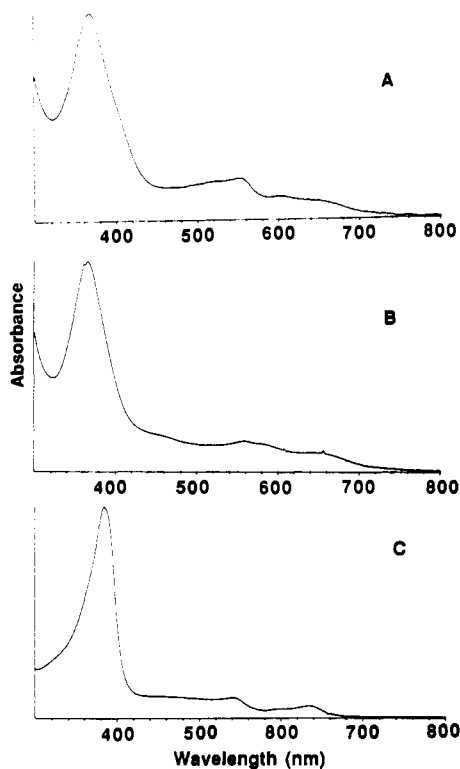


Figure 1. UV/vis absorption spectra of dichloromethane solutions of (A) (OEAP)Fe^{III}Cl, (B) (HOEAP)Fe^{III}Cl₂ formed from (OEAP)Fe^{III}Cl and excess hydrogen chloride, and (C) [(OEAP)Fe^{III}(DMSO)₂](NO₃) in DMSO solution.

frozen dichloromethane at 5 K shows a typical high-spin pattern with features at $g = 5.8$ and $g = 2.0$.

Crystal and Molecular Structure of (OEAP)Fe^{III}Cl·CH₂Cl₂·N₂. The compound crystallized with the azaporphyrin complex, a molecule of dichloromethane, and a dinitrogen molecule in the asymmetric unit. Two views of the azaporphyrin complex are given in Figure 2. Atomic positional parameters are presented in Table I. Table II gives a listing of important bond distances and angles.

The location of the meso nitrogen within the macrocycle has been achieved through comparison of the local electron density. Additionally, the methine hydrogens bound to C(2), C(17), and C(11) have all been located but no evidence for electron density corresponding to a proton on N(5) was observed. There is a molecule of dichloromethane which is near the meso nitrogen bridge. Its location can be seen by examining the lower part of Figure 2. The H...N distance is 2.98 Å. The C(CH₂Cl₂)-H...N angle is 120°, and the C(pyrrole)-H...N angles are 87.5 and 81.7°. These contacts suggest that there is a weak hydrogen bond formed between these molecules.

As expected, the C-N distances (average 1.361 Å) at the meso nitrogen are slightly shorter than the C-C distances (average 1.375 Å) at the methine bridges. The structural study of (13,17-diethyl-2,3,7,8,12,18-hexamethyl-5-azaporphyrinato)cobalt(II) showed a somewhat larger difference in the C-N distances (average 1.33 Å) at the meso nitrogen versus the C-C distances (1.38 Å) at the methine bridge.¹²

The iron is five-coordinate. Its structural parameters are consistent with the parameters observed for high-spin, five-coordinate iron(III) porphyrins.^{14,15} The Fe-N distances (average 2.044 Å) are just slightly shorter than the range (2.060–2.087 Å) found for analogous porphyrin complexes. The distance from the iron ion to the center of the plane of the four nitrogen atoms

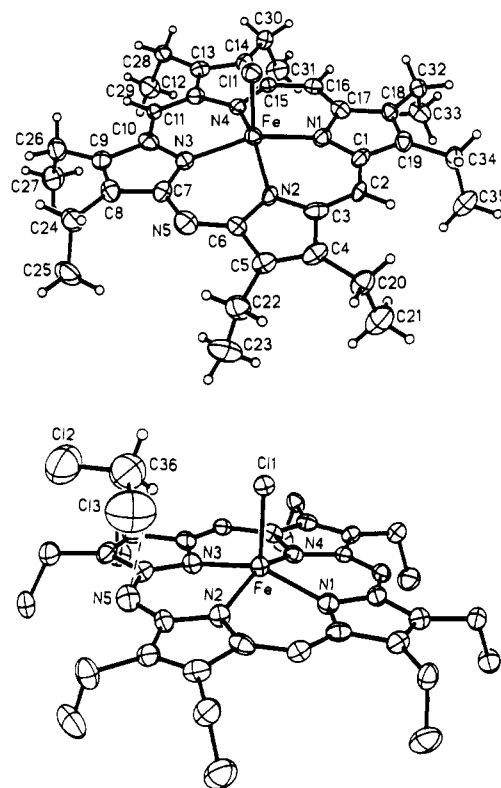


Figure 2. Perspective views of (OEAP)Fe^{III}Cl with 50% thermal contours for all atoms.

is 0.49 Å, and the distance of the iron to the center of the porphyrin mean plane is 0.54 Å. In corresponding porphyrin complexes the ranges of these distances are 0.39–0.54 and 0.39–0.62 Å, respectively.

Figure 3 shows the out-of-plane displacements of the iron and the azaporphyrin core. In order to accommodate the five-coordinate iron, the porphyrin is slightly domed.

¹H NMR Spectral Studies. The ¹H NMR spectrum of (OEAP)Fe^{III}Cl in dichloromethane at 23 °C is shown in trace A of Figure 4. Resonances have been assigned on the basis of their intensities and line widths. The meso resonances are expected to be the broadest if dipolar relaxation is operative, since they are closest to the paramagnetic iron center. Consequently, the two upfield resonances with intensities appropriate for 2 and 1 protons are assigned to the meso protons. The eight equally intense resonances in the 39–49 ppm region have nearly the same line widths. These are assigned to the methylene protons. The three resonances in the 7–8 ppm region are assigned to the methyl protons. The highest field one of these is more intense than the other two and appears to correspond to four methyl groups, while each of the others results from equivalent pairs of methyl groups.

Treatment of a dichloromethane-*d*₂ solution of (OEAP)Fe^{III}Cl with hydrogen chloride produces a marked change in the ¹H NMR spectrum. Figure 5 shows the spectrum obtained at –78 °C. This temperature was chosen because it produces a well-resolved spectrum. The complex is stable to warming to 23 °C. The two broad resonances at 46 and 22 ppm with a 1:2 intensity ratio are readily assigned as the meso protons. The four equally intense resonances in the 90–60 ppm region are assigned to the methylene protons. The resonances at 12 and 10 ppm are assigned to the methyl protons. The upfield resonance at –46 ppm is assigned to the N-H group at the meso nitrogen. This assignment has been verified by deuterium labeling. When (OEAP)Fe^{III}Cl is treated with deuterium chloride, this upfield resonance cannot be observed.

Figure 6 shows the ¹H NMR spectrum obtained from a solution of (OEAP)Fe^{III}Cl in dimethyl-*d*₆ sulfoxide after treatment with

(14) Scheidt, W. R.; Reed, C. A. *Chem. Rev.* **1981**, *81*, 543.

(15) Scheidt, W. R.; Lee, Y. J. *Struct. Bonding* **1987**, *64*, 1.

Table I. Atomic Coordinates ($\times 10^4$) and Equivalent Isotropic Displacement Coefficients ($\text{\AA}^2 \times 10^3$) for (OEAP)Fe^{III}Cl·CH₂Cl₂·N₂

	x	y	z	U(eq) ^a
Fe	2481 (1)	1250 (1)	1752 (1)	25 (1)
Cl(1)	4174 (2)	2207 (2)	1191 (2)	29 (1)
N(1)	3516 (7)	-315 (5)	2122 (5)	29 (3)
N(2)	2234 (7)	950 (5)	3238 (5)	26 (3)
N(3)	742 (7)	2406 (5)	1638 (5)	26 (3)
N(4)	1947 (6)	1151 (5)	503 (5)	25 (3)
C(1)	4149 (9)	-936 (7)	2981 (6)	29 (4)
C(2)	3929 (8)	-718 (6)	3832 (6)	25 (4)
C(3)	3006 (9)	146 (7)	3950 (6)	31 (4)
C(4)	2705 (9)	295 (7)	4901 (6)	34 (4)
C(5)	1729 (9)	1209 (7)	4724 (6)	31 (4)
C(6)	1449 (8)	1615 (7)	3697 (6)	29 (4)
N(5)	551 (8)	2555 (6)	3250 (6)	41 (4)
C(7)	225 (8)	2926 (7)	2294 (7)	29 (4)
C(8)	-771 (9)	3879 (7)	1851 (7)	33 (4)
C(9)	-921 (8)	3965 (7)	917 (7)	30 (4)
C(10)	59 (8)	3031 (7)	792 (7)	30 (4)
C(11)	237 (8)	2822 (6)	-57 (6)	24 (4)
C(12)	1116 (8)	1931 (7)	-194 (6)	28 (4)
C(13)	1217 (8)	1678 (7)	-1068 (6)	27 (4)
C(14)	2177 (8)	726 (6)	-894 (6)	26 (4)
C(15)	2623 (8)	405 (6)	75 (6)	22 (4)
C(16)	3569 (8)	-504 (6)	526 (6)	26 (4)
C(17)	4010 (8)	-856 (7)	1469 (7)	27 (4)
C(18)	4977 (8)	-1827 (7)	1947 (6)	27 (4)
C(19)	5070 (8)	-1890 (7)	2883 (7)	29 (4)
C(20)	3341 (10)	-476 (7)	5858 (6)	38 (4)
C(21)	2623 (12)	-1413 (8)	6366 (8)	58 (5)
C(22)	976 (9)	1705 (8)	5452 (7)	43 (5)
C(23)	-383 (11)	1371 (9)	5830 (8)	65 (6)
C(24)	-1472 (9)	4650 (7)	2353 (7)	41 (4)
C(25)	-2688 (10)	4283 (8)	3067 (8)	54 (5)
C(26)	-1881 (9)	4759 (7)	172 (7)	40 (4)
C(27)	-3151 (9)	4333 (8)	209 (7)	49 (5)
C(28)	422 (8)	2347 (7)	-1960 (6)	31 (4)
C(29)	-999 (9)	2087 (8)	-1816 (7)	44 (5)
C(30)	2616 (9)	91 (6)	-1545 (6)	31 (4)
C(31)	1827 (10)	-823 (7)	-1268 (7)	47 (5)
C(32)	5688 (8)	-2622 (7)	1480 (7)	30 (4)
C(33)	4816 (9)	-3402 (7)	1516 (7)	38 (4)
C(34)	5896 (9)	-2770 (7)	3696 (6)	33 (4)
C(35)	5066 (9)	-3568 (7)	4399 (7)	50 (5)
C(36)	3316 (12)	3971 (10)	2533 (9)	77 (7)
Cl(2)	2043 (3)	5046 (3)	2522 (3)	94 (2)
Cl(3)	3905 (4)	3137 (3)	3648 (3)	102 (3)
N(6)	1370 (13)	5624 (12)	4900 (10)	102 (8)
N(7)	865 (14)	4822 (12)	5240 (12)	127 (9)

^a Equivalent isotropic *U* defined as one-third of the trace of the orthogonalized *U_{ij}* tensor.

silver nitrate. This yields [(OEAP)Fe^{III}(DMSO-*d*₆)₂](NO₃)₃.¹³ The broad resonance at 36.5 ppm is assigned to the meso protons on the basis of its line width. No other broad resonance was observed. The two meso resonances due to protons *m* and *m'* may be accidentally degenerate, or the other meso resonance may lie under the resonances in the 28–32 ppm region or in the 0–5 ppm region. The three resonances in the 28–32 ppm region are assigned to the methylene protons, with the resonance at 29 ppm resulting from the accidental degeneracy of two methyl resonances. On warming, the line widths decrease and resolution improves. Inset B shows a portion of the spectrum that was acquired at 80 °C. At that temperature the four individual methylene resonances are clearly resolved. The two resonances in the 4–6 ppm range are assigned to the methyl protons.

Similarly, treatment of (OEP)Fe^{III}Cl with dimethyl sulfoxide and silver nitrate yields a solution of [(OEP)Fe^{III}(DMSO-*d*₆)₂](NO₃)₃, which has a broad meso resonance at 40 ppm, a methylene resonance at 47.3 ppm, and a methyl resonance at 7 ppm at 19 °C.

Discussion

The crystallographic work indicates that the azaporphyrin ligand acts much like a porphyrin in forming a high-spin, five-

Table II. Selected Bond Lengths (Å) and Angles (deg) for (OEAP)Fe^{III}Cl·CH₂Cl₂·N₂

Bond Lengths			
Fe-Cl(1)	2.254 (3)	Fe-N(1)	2.042 (7)
Fe-N(2)	2.042 (7)	Fe-N(3)	2.035 (6)
Fe-N(4)	2.058 (8)	N(1)-C(1)	1.367 (10)
N(1)-C(17)	1.399 (13)	N(2)-C(3)	1.357 (9)
N(2)-C(6)	1.371 (12)	N(3)-C(7)	1.384 (13)
N(3)-C(10)	1.376 (10)	N(4)-C(12)	1.365 (9)
N(4)-C(15)	1.396 (12)	C(1)-C(2)	1.372 (14)
C(1)-C(19)	1.454 (12)	C(2)-C(3)	1.371 (12)
C(3)-C(4)	1.467 (14)	C(4)-C(5)	1.354 (12)
C(5)-C(6)	1.436 (13)	C(6)-N(5)	1.366 (10)
N(5)-C(7)	1.357 (12)	C(7)-C(8)	1.427 (10)
C(8)-C(9)	1.362 (15)	C(9)-C(10)	1.474 (12)
C(10)-C(11)	1.365 (15)	C(11)-C(12)	1.391 (12)
C(12)-C(13)	1.442 (15)	C(13)-C(28)	1.492 (11)
C(14)-C(30)	1.490 (14)	C(15)-C(16)	1.368 (10)
C(16)-C(17)	1.384 (13)	C(17)-C(18)	1.435 (10)
C(18)-C(19)	1.361 (14)		
Bond Angles			
Cl(1)-Fe-N(1)	103.3 (2)	Cl(1)-Fe-N(2)	103.9 (2)
N(1)-Fe-N(2)	86.9 (3)	Cl(1)-Fe-N(3)	103.5 (2)
N(1)-Fe-N(3)	153.1 (3)	N(3)-Fe-N(3)	85.9 (3)
Cl(1)-Fe-N(4)	104.4 (2)	N(1)-Fe-N(4)	87.6 (3)
N(2)-Fe-N(4)	151.7 (3)	N(3)-Fe-N(4)	86.5 (3)
Fe-N(1)-C(1)	125.9 (7)	Fe-N(1)-C(17)	126.3 (5)
C(1)-N(1)-C(17)	106.0 (7)	Fe-N(2)-C(3)	126.2 (6)
Fe-N(2)-C(6)	127.3 (5)	C(3)-N(2)-C(6)	105.5 (7)
Fe-N(3)-C(7)	126.7 (6)	Fe-N(3)-C(10)	126.5 (6)
C(7)-N(3)-C(10)	104.8 (7)	Fe-N(4)-C(12)	126.8 (7)
Fe-N(4)-C(15)	125.8 (5)	C(12)-N(4)-C(15)	105.6 (7)
N(1)-C(1)-C(2)	125.4 (7)	N(1)-C(1)-C(19)	110.4 (8)
C(2)-C(1)-C(19)	124.2 (7)	C(1)-C(2)-C(3)	124.6 (7)
N(2)-C(3)-C(4)	126.0 (9)	N(2)-C(3)-C(4)	111.1 (8)
C(2)-C(3)-C(4)	122.9 (7)	C(3)-C(4)-C(5)	105.2 (7)
C(4)-C(5)-C(6)	107.6 (9)	N(2)-C(6)-C(5)	110.7 (6)
N(2)-C(6)-N(5)	125.8 (8)	C(5)-C(6)-N(5)	123.5 (9)
C(6)-N(5)-C(7)	124.3 (9)	N(3)-C(7)-N(5)	125.2 (7)
N(3)-C(7)-C(8)	111.0 (8)	N(5)-C(7)-C(8)	123.8 (9)
C(7)-C(8)-C(9)	108.4 (9)	C(8)-C(9)-C(10)	104.7 (7)
N(3)-C(10)-C(9)	111.2 (9)	N(3)-C(10)-C(11)	125.4 (8)
C(9)-C(10)-C(11)	123.4 (7)	C(10)-C(11)-C(12)	125.2 (7)
N(4)-C(12)-C(11)	124.2 (9)	N(4)-C(12)-C(13)	111.1 (7)
C(11)-C(12)-C(13)	124.6 (7)	C(12)-C(13)-C(14)	106.0 (7)
C(13)-C(14)-C(15)	107.2 (8)	N(4)-C(15)-C(16)	110.1 (6)
N(4)-C(15)-C(16)	124.7 (8)	C(14)-C(15)-C(16)	125.2 (9)
C(15)-C(16)-C(17)	127.1 (9)	N(1)-C(17)-C(16)	123.7 (7)
N(1)-C(17)-C(18)	109.5 (8)	C(16)-C(17)-C(18)	126.8 (9)
C(17)-C(18)-C(19)	107.7 (8)	C(1)-C(19)-C(18)	106.4 (7)

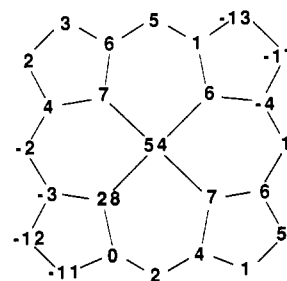


Figure 3. Diagram of the azaporphyrin core of (OEAP)Fe^{III}Cl. Each atom symbol has been replaced by a number that represents the perpendicular displacement, in units of 0.01 Å, of that atom from the mean plane of the azaporphyrin.

coordinate iron complex with an axial chloride ligand. The solid state structure is unusual for a core modified with symmetrical peripheral substitution because it is fully ordered. Modification of a porphyrin in the interior core generally results in small geometric changes in the interior of the molecule. These generally do not effect a major alteration to the external shape of the molecule. Consequently, the forces that are responsible for crystal formation frequently do not discriminate between essentially equivalent orientations of the molecule. Thus, disorder has been

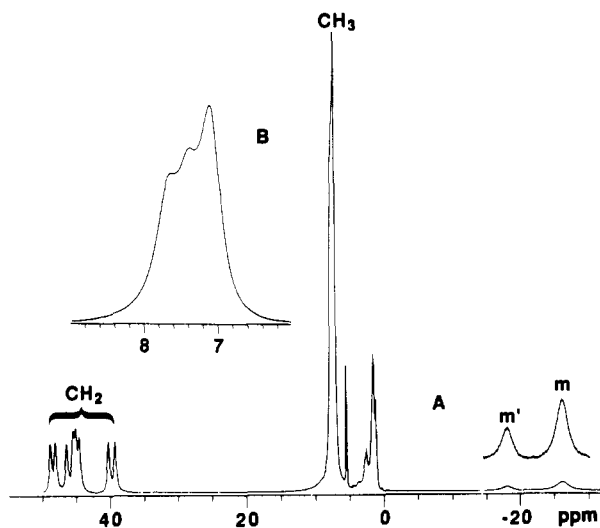


Figure 4. (A) 300-MHz ^1H NMR spectrum of $(\text{OEAP})\text{Fe}^{\text{III}}\text{Cl}$ in dichloromethane- d_2 solution at 23 $^\circ\text{C}$. Resonance labels: m, m' = meso protons; CH_2 = methylene protons; CH_3 = methyl protons. (B) An expansion of the region of the resonances assigned to the methyl protons.

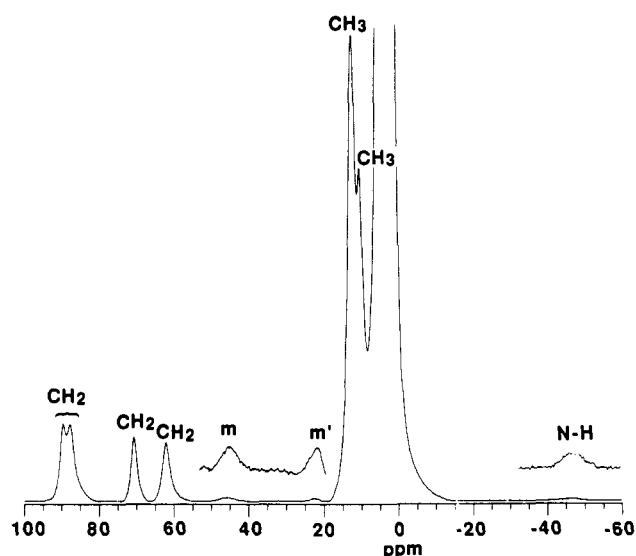


Figure 5. 300-MHz ^1H NMR spectrum of $(\text{HOEAP})\text{Fe}^{\text{III}}\text{Cl}_2$ formed by treating $(\text{OEAP})\text{Fe}^{\text{III}}\text{Cl}$ with hydrogen chloride in dichloromethane- d_2 at -78 $^\circ\text{C}$.

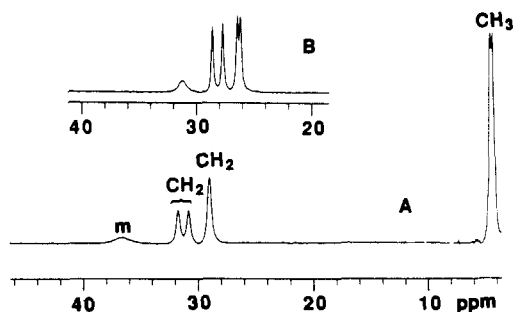


Figure 6. (A) 300-MHz ^1H NMR spectrum of $[(\text{OEAP})\text{Fe}^{\text{III}}(\text{DMSO}-d_6)_2](\text{NO}_3)$ in dimethyl- d_6 sulfoxide at 23 $^\circ\text{C}$. Resonances are labeled in accord with Figure 4. (B) A portion of the spectrum at 80 $^\circ\text{C}$.

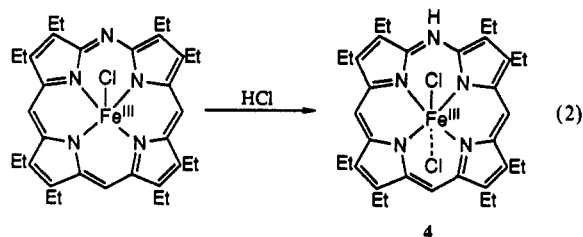
seen in the crystal structures of other core-modified porphyrins: octaethylporphyrin *N*-oxide,¹⁶ *meso*-tetraphenylthiaporphyrin,^{17,18} (octaethylxophlorin radical)zinc(II)-pyridine,¹⁹ and octaethylxoporphylin complexes of iron.⁵ In the case of

(16) Balch, A. L.; Chan, Y. W.; Olmstead, M. M.; Renner, M. W. *J. Am. Chem. Soc.* **1985**, *107*, 2393.

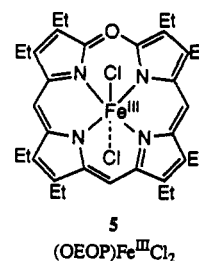
$(\text{OEAP})\text{Fe}^{\text{III}}\text{Cl}\cdot\text{CH}_2\text{Cl}_2\cdot\text{N}_2$, it appears that the hydrogen-bond interaction between the meso nitrogen and the dichloromethane molecule contributes to the formation of an ordered structure.

The ^1H NMR spectrum of $(\text{OEAP})\text{Fe}^{\text{III}}\text{Cl}$ indicates that it retains its structure in noncoordinating solvents. The spectrum shown in Figure 4 shows eight distinct methylene resonances. Thus each proton of the four methylene groups (a-d in structure 3) is unique because the iron is five-coordinate. The overall pattern of resonances for $(\text{OEAP})\text{Fe}^{\text{III}}\text{Cl}$ is similar to that of the porphyrin complex $(\text{OEP})\text{Fe}^{\text{III}}\text{Cl}$. The latter has its meso resonance upfield at -56.1 ppm, two methylene resonances downfield at 44.5 and 40.9 ppm, and the methyl resonance at 6.7 ppm in dichloromethane at 25 $^\circ\text{C}$.²⁰ Consequently the two complexes must have grossly similar electronic structures. Aside from the lower symmetry of the azaporphyrin, the major difference between them is in the meso shifts, which are considerably further upfield for the porphyrin complex than for the azaporphyrin complex.

Addition of hydrogen chloride to $(\text{OEAP})\text{Fe}^{\text{III}}\text{Cl}$ converts it into a more symmetrical species, as the ^1H NMR spectra clearly show. The product is formulated as $(\text{HOEAP})\text{Fe}^{\text{III}}\text{Cl}_2$ (4) (see eq 2). In this six-coordinate structure with two identical axial



ligands, the methylene protons of each ethyl group are equivalent, and hence there are four rather than eight methylene resonances. The N-H resonance of the meso nitrogen has been observed and its assignment verified by deuterium labeling. Complex 4 is isoelectronic with the oxoporphylin complex 5, which was recently isolated and characterized crystallographically.⁵ The ^1H NMR patterns of 4 and 5 are similar.



Reaction 2 emphasizes a novel aspect of the chemistry of the azaporphyrin ligand. The ability of the meso nitrogen to accept a proton switches the ligand from a dianionic tetradentate ligand with porphyrin-like characteristics to a monoanionic ligand with characteristics that are similar to those of the oxoporphyryns. This manifests itself in a facile change in coordination numbers in reaction 2. Similar behavior can be expected to occur when the meso nitrogen of azaporphyrin is alkylated.

Another high-spin, six-coordinate complex $[(\text{OEAP})\text{Fe}^{\text{III}}(\text{DMSO})_2]^+$, has also been obtained. Its ^1H NMR spectrum, like that of $(\text{HOEAP})\text{Fe}^{\text{III}}\text{Cl}_2$, shows four equally intense

(17) Latos-Grażyński, L.; Lisowski, J.; Olmstead, M. M.; Balch, A. L. *J. Am. Chem. Soc.* **1987**, *109*, 4428.

(18) Latos-Grażyński, L.; Lisowski, J.; Sztrenberg, L.; Olmstead, M. M.; Balch, A. L. *J. Org. Chem.* **1991**, *56*, 4043.

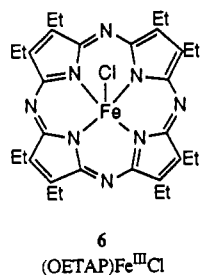
(19) Balch, A. L.; Noll, B. C.; Zovinka, E. P. *J. Am. Chem. Soc.* **1992**, *114*, 3380.

(20) Morishima, I.; Kitagawa, S.; Matsuki, E.; Inubushi, T. *J. Am. Chem. Soc.* **1980**, *102*, 2429.

methylene resonances. Its meso proton resonance is downfield rather than upfield as seen for five-coordinate (OEAP)Fe^{III}Cl.

With iron(III) porphyrin complexes, the chemical shift of the meso proton has been shown to be a useful diagnostic probe that can distinguish between five- and six-coordination geometries for high-spin complexes.^{13,21,22} Five-coordinate, high-spin complexes have upfield meso proton resonances as described above for (OEP)Fe^{III}Cl. In contrast, six-coordinate, high-spin complexes have downfield chemical shifts for the meso proton resonances. The same pattern holds for the azaporphyrin complexes considered here. Five-coordinate (OEP)Fe^{III}Cl has both of the meso resonances in upfield positions. In contrast, both (HOEAP)-Fe^{III}Cl₂ and [(OEAP)Fe^{III}(DMSO)₂]⁺ have meso C-H resonances in downfield positions.

Recently, the preparation and characterization of iron complexes of octaethyltetraazaporphyrins were reported.²³ The properties of the iron(III) complex **6**, (OETAP)Fe^{III}Cl, are of relevance



for comparison with **3**. The tetraazaporphyrin is even more constricted in its hole size than is the monoazaporphyrin. As a consequence, the average Fe-N distance in **6** (1.929 (7) Å) is shorter than the average Fe-N distance **3** (2.044 (7) Å) and the iron(III) ion in **6** is displaced only 0.352 (3) Å from the N₄ plane, whereas it is 0.49 Å out of that plane in **3**. These structural differences parallel differences in magnetic properties. The tetraaza complex **6** has been shown to possess a unusual, intermediate-spin ($S = 3/2$) ground state²³ whereas **6** is a high-spin ($S = 5/2$) species, which is typical of iron(III) porphyrin complexes with one axial, anionic ligand.

Experimental Section

Preparation of Compounds. Octaethylporphyrin was purchased from Aldrich.

(OEAP)Fe^{III}Cl. This was obtained by a modification of the previously described route.¹¹ A 500-mg sample of ascorbic acid was added to a solution of 100 mg of (OEP)Fe^{II}(py)₂ in 6 mL of pyridine. A 50-mL portion of dichloromethane which was saturated with dioxygen was added. The mixture was shaken for 5 min. The green solution was filtered to remove any insoluble material, and the filtrate was washed with two 50-mL portions of water. The resulting green solution was dried by passing it through a 5 cm thick bed of anhydrous sodium sulfate. The sample was evaporated to dryness under vacuum to give a green, air-sensitive residue, which was handled in a dioxygen-free environment. The solid was dissolved in 20 mL of dioxygen-free dichloromethane. A sample of 30 mL of dioxygen-free *n*-hexane was added. The volume of the sample was reduced under vacuum until a green precipitate formed. At this stage, an additional 10-mL portion of *n*-hexane was added. The deep green precipitate of verdohemochrome (**2**, X=Cl) (yield 52 mg) was collected by filtration and washed with *n*-hexane to remove a brown substance. The electronic spectrum of this material (λ_{max} , nm (ϵ , cm⁻¹ M⁻¹): 384 (6.5 × 10⁴), 494 (9.2 × 10³), 526 (1.7 × 10⁴), 651 (5.5 × 10⁴) agrees with those of previous verdohemochrome preparations.²⁻⁴

Concentrated ammonium hydroxide (10 mL) was added to a solution of 50 mg (0.06 mmol) of verdohemochrome (**2**) in 15 mL of pyridine.

Table III. Crystallographic Data for (OEAP)Fe^{III}Cl·CH₂Cl₂·N₂

C ₃₆ H ₄₅ Cl ₃ FeN ₇	fw = 738.0
<i>a</i> = 10.051 (2) Å	P $\bar{1}$, triclinic
<i>b</i> = 13.746 (3) Å	<i>T</i> = 130 K
<i>c</i> = 14.712 (3) Å	λ (Cu K α) = 1.541 84 Å
α = 66.50 (3)°	μ = 5.678 mm ⁻¹
β = 80.72 (3)°	d_{calcd} = 1.359 Mg/m ³
γ = 75.93 (3)°	transm factors = 0.60–0.83
<i>V</i> = 1803.4 (6) Å ³	<i>R</i> (<i>F</i>) ^a = 0.071
<i>Z</i> = 2	<i>R</i> _w (<i>F</i>) ^a = 0.089

$$^a R = \sum ||F_o| - |F_c|| / \sum |F_o|; R_w = \sum ||F_o| - |F_c||w^{1/2} / \sum |F_o|w^{1/2}; w^{-1} = \sigma^2 |F| + 0.0013F^2.$$

This mixture was stirred for 10 h and then diluted with 50 mL of water. The mixture was extracted in two 50-mL portions of dichloromethane. The dichloromethane solutions were combined, washed with two 50-mL portions of water, and dried over anhydrous sodium sulfate. The solution was evaporated to dryness, and the dark residue was dissolved in 100 mL of 5% sulfuric acid in methanol. The mixture was allowed to stand for 5 h, and then 30 mL of water was added. This solution was extracted with three 50-mL portions of dichloromethane. The combined extracts were washed with two 50-mL portions of water, dried over sodium sulfate, and evaporated to dryness. The residue was dissolved in dichloromethane and subjected to chromatography on a silical gel column. Elution with dichloromethane/methanol (50/1 v/v) produced a red and a blue band. Further elution with dichloromethane/methanol (1/1 v/v) produced a greenish brown band, which was collected and evaporated to dryness. The residue was dissolved in 20 mL of 2% hydrochloric acid in methanol. After 2 min of standing, the solution was evaporated to dryness under vacuum. The reddish brown solid was purified by recrystallization from dichloromethane/petroleum ether (yield 13.8 mg, 35%). The UV/vis absorption spectrum is shown in Figure 1, and the ¹H NMR spectrum is reproduced in Figure 4.

[(OEAP)Fe^{III}(DMSO-*d*₆)₂](NO₃). A 5-mg (0.008-mmol) portion of (OEAP)Fe^{III}Cl was dissolved in 1 mL of dimethyl-*d*₆ sulfoxide. Silver nitrate (13.5 mg, 0.08 mmol) was added as a solid. The sample was stirred for 2 h and then filtered. The filtrate was used for spectroscopic characterization of the complex (Figure 5). Attempts to isolate the complex as a solid were not successful. A similar procedure with (OEP)-Fe^{III}Cl was used to form [(OEP)Fe^{III}(DMSO-*d*₆)₂](NO₃).

(HOEAP)Fe^{III}Cl₂. A 5-mg portion of (OEAP)Fe^{III}Cl was dissolved in 1 mL of dichloromethane-*d*₂. Hydrogen chloride vapor was added to the solution to produce solutions for spectroscopic study. Attempts to isolate the product were frustrated by conversion back to (OEAP)Fe^{III}Cl when the excess hydrogen chloride was removed.

X-ray Data Collection for (OEAP)Fe^{III}Cl·CH₂Cl₂·N₂. Red blocks were obtained by diffusion of petroleum ether into a dichloromethane solution of the complex. A suitable crystal was coated with a light hydrocarbon oil and mounted in the 130 K dinitrogen stream of a Siemens P4/RA diffractometer equipped with a Siemens LT-2 low-temperature apparatus. Two check reflections showed random (<2%) variation during data collection. The data were corrected for Lorentz and polarization effects. Crystal data are given in Table III.

Solution and Refinement of the Structure. Calculations were performed on a DEC VAX station 3200 with the programs of SHELXTL Plus v. 4.21. Scattering factors for neutral atoms and corrections for anomalous dispersion were taken from a standard source.²⁴ An absorption correction was applied to the structure.²⁵ The solution of the structure was obtained by direct methods. During the last stages of refinement all non-hydrogen atoms were assigned anisotropic thermal parameters. Hydrogen atoms were located on a difference map and fixed at ideal geometries for subsequent cycles of least-squares refinement. The molecule of dinitrogen is unusual, but no other explanation for two equal-sized atoms separated by 1.21 (2) Å could be found. We are aware of one other case where a molecule of dinitrogen has been found as an occlusion in the crystalline form of a metal complex.²⁶ There is a close contact (1.86 Å) between two such molecules in the structure which forms the angle N-N-N of 109°. There are no other short contacts to other portions of the structure.

(21) Morishima, I.; Shiro, Y.; Wakino, T. *J. Am. Chem. Soc.* **1985**, *107*, 1063.

(22) Rajarathnam, K.; La Mar, G. N.; Chiu, M. L.; Sligar, S. G.; Singh, J. P.; Smith, K. M. *J. Am. Chem. Soc.* **1991**, *113*, 7886.

(23) Fitzgerald, J. P.; Haggerty, B. S.; Rheingold, A. L.; May, L.; Brewer, G. A. *Inorg. Chem.* **1992**, *31*, 2006.

(24) *International Tables for X-ray Crystallography*; Kynoch Press: Birmingham, England, 1974; Vol. 4.

(25) The method obtains an empirical absorption from an expression relating *F*_o and *F*_c; Moezzi, B. Ph.D. Thesis, University of California, Davis, 1987.

(26) Wood, F. E.; Olmstead, M. M.; Balch, A. L. *J. Am. Chem. Soc.* **1983**, *105*, 6332.

Instrumentation. ^1H NMR spectra were recorded on a General Electric QE-300 FT NMR spectrometer operating in the quadrature mode (^1H frequency is 300 MHz). The spectra were collected over a 50-kHz bandwidth with 16K data points and a 5- μs 45° pulse. For a typical spectrum, between 1000 and 5000 transients were accumulated with a 50-ms delay time. The signal to noise ratio was improved by apodization of the free induction decay. Electronic spectra were obtained using a Hewlett Packard diode array spectrometer. ESR spectra were obtained using a Bruker spectrometer. The magnetic moment of **3** was measured by the Evans technique.²⁷

Acknowledgment. We thank the National Institutes of Health (Grant GM-26226) for financial support.

Supplementary Material Available: Tables of all bond lengths, bond angles, anisotropic thermal parameters, hydrogen atom positions, and data collection parameters for $(\text{OEAP})\text{Fe}^{\text{III}}\text{Cl}\cdot\text{CH}_2\text{Cl}_2\cdot\text{N}_2$ (7 pages). Ordering information is given on any current masthead page.

(27) Evans, D. F. *J. Chem. Soc.* **1959**, 2003.